A hair ribbon deflection model for low-intrusiveness measurement of bow force in violin performance

Marco Marchini[†]
marco.marchini@upf.edu

Panos Papiotis[†]
panos.papiotis@upf.edu

Alfonso Pérez[†]
alfonso.perez@upf.edu

Esteban Maestre[†‡]
esteban.maestre@upf.edu
esteban@ccrma.stanford.edu

[†] Music Technology Group, Universitat Pompeu Fabra, Barcelona, Spain
[‡] Center for Computer Research in Music and Acoustics, Stanford University, USA

ABSTRACT

This paper introduces and evaluates a novel methodology for the estimation of bow pressing force in violin performance, aiming at a reduced intrusiveness while maintaining high accuracy. The technique is based on using a simplified physical model of the hair ribbon deflection, and feeding this model solely with position and orientation measurements of the bow and violin spatial coordinates. The physical model is both calibrated and evaluated using real force data acquired by means of a load cell.

Keywords

bow pressing force, bow force, pressing force, force, violin playing, bow simplified physical model, 6DOF, hair ribbon ends, string ends

1. INTRODUCTION

Violin is regarded as among the most complex musical instruments, making different control parameters available for the performer to freely shape rich timbre characteristics of produced sound. Within the different bowing control parameters, only the bow transversal velocity could be considered as of comparable importance as the bow pressing force exerted by the player on the string [2]. When approaching the study of violin performance from a computational perspective, the accurate acquisition of control parameter signals appears as highly desirable, as it has been demonstrated by the research effort devoted to such pursuit during the past few years [1, 12, 7, 3, 5, 8]. In particular, the measurement of bow pressing force not only has received special attention because of its key role in timbre control, but also because of a number of measurement-specific issues that appear as harder to overcome, as it is accuracy, robustness, or intrusiveness.

An early attempt to pursue the measurement of bow pressing force from real violin practice dates back to 1986. Askenfelt [1] used wired strain gages at the frog and the tip in order to infer the bow pressing force applied on the string. Although useful for the instrument-modeling purposes of the authors, significant intrusiveness would make difficult the use of such a system in a real performance scenario.

Intrusiveness improved significantly by a first wireless acquisition system proposed by Paradiso [8], who attached a resistive strip to the bow which was driven by an antenna mounted behind the bridge of the cello. A measurement relative to the bow pressing force was carried out by using a force-sensitive resistor below the forefinger. Despite the reduction on intrusiveness, the obtained measure resulted rather unrelated to the actual force exerted on the string, as it happened to Young's approach [12], who measured downward and lateral bow pressure with foil strain gages permanently mounted around the midpoint of the bow stick.

The first effort to relate the strain of the bow hair as a measure of force was carried out by Rasamimanana [9], although the technique reached its first state of maturity (in terms of accuracy) with the technique introduced by Demoucron [4] and more recently reused and improved by Guaus [5]: the deflection of the hair ribbon is measured at the frog (and also at the tip in one of the earlier versions) by using a strain gage attached to a plate laying against the hair ribbon which bends when the string is pressed. This technique, while providing surprisingly good estimations of bow force, suffers from remarkable intrusiveness and reduced robustness, making difficult its prolonged use in stage or performance contexts.

In this paper, we present a methodology for the estimation of bow pressing force by using a simplified physical model of the hair ribbon deflection which makes use of only position and orientation (6DOF) measurements on the bow and violin. The motivation is to minimize the intrusiveness by avoiding the use of additional sensors, and therefore construct a more reliable system that can be used more naturally for longer periods of time. The principal source of information comes from measuring, as it was already proposed by Maestre [7], the distance between the ideal (no deflection) segment defined by the ends of the hair ribbon, and the segment defined by the ends of the string being played. A physical model of the hair ribbon deflection is constructed and calibrated from real data measurements using a load cell, and used later for estimating the bow force in real performances.

The rest of the paper remains as follows. Section 2 introduces the measurement system and outlines the features used in our study. In Section 3 we present a simplified physical model for a single hair thread and then generalize it to describe the complete hair ribbon. Section 4 describes a procedure to minimize the deviation between our model and recorded force data. We conclude with some prelimi-

NIME'11, 30 May–1 June 2011, Oslo, Norway.

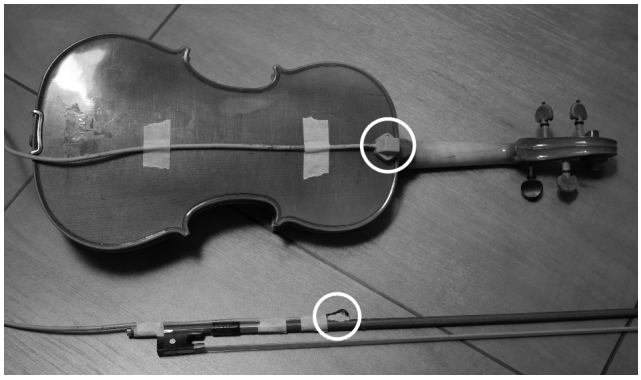

Figure 1: Detail of violin and bow placement of sensors during a performance recording.

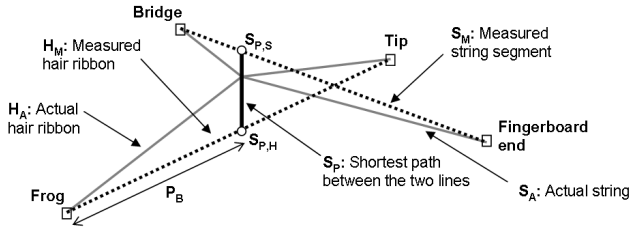

Figure 2: Measured string and hair ribbon segments, computed from their extracted end points, versus their actual configuration. Deformations have been exaggerated in order to illustrate the importance of segment S_P .

nary results along with future directions.

2. MEASUREMENT SYSTEM

To obtain the physical parameters necessary for the estimation of vertical bow force against the violin string, we utilize the methodology described in [5, 7]. Essentially, the methodology consists in (i) acquiring instrumental gesture parameters (such as bow transversal position and hair ribbon-to-violin string distance), and (ii) using a load cell to measure applied force during calibration and evaluation.

2.1 Acquisition of violin instrumental gesture parameters

The acquisition of the instrumental gesture parameters is done in real-time using the Polhemus Liberty system[1], a 6DOF tracking system based on electromagnetic field sensing (EMF), and consisting of two wired miniature sensors and a transmitting source. Each sensor provides three 3DOF for position and 3DOF for orientation, both at 240Hz sampling rate, with static accuracies of 0.75mm and 0.15 degrees RMS respectively. These sensors are respectively placed on the bow and the body of the violin, as seen in Figure 1. From the position and orientation data provided by these two sensors, and thanks to a calibration procedure involving a third sensor, we are able to obtain the position of the ends of the strings, and the (ideal, assuming no deformation) position of of the four ends of the hair ribbon (considered as having finite width), as detailed in [7].

Having obtained the position of the strings as well as the bow hair ribbon, we can proceed to calculate several parameters regarding the position and orientation of the bow with respect to the violin strings (see Figure 2). Particularly for this model, the most relevant parameters are:

1. **bow transversal position**, also referred to as *bow displacement*; this is is computed as the euclidean distance between $S_{P,H}$ and the measured frog end of the hair ribbon.

2. **bow-string distance**, also referred to as *pseudo-force*; the modulus of the intersecting line segment S_P , which is perpendicular to the string and to the hair ribbon. This segment will get longer for higher deformations due to pressing force. Thus, we compute a euclidean distance between $S_{P,S}$ and $S_{P,H}$ between each of the two longitudinal edges (left, right) of the hair ribbon (tracked as a finite surface instead of as it is shown in Figure 2 for the sake of simplicity).

[1] `www.polhemus.com`

2.2 Measurement of applied force

In order to both design and evaluate our system, we used a linear load cell to measure the actual force being applied by the bow, as suggested by [10] and implemented in [5]. The cell is fixed to a wooden support, while a thin methacrylate cylinder is placed over the cell to simulate a virtual string. By using a similar calibration method described above, we are able to track the ends of the cylinder and thus acquire a number of bowing parameters (including *bow displacement* and *pseudoforce* as simultaneously recorded along with the output of the load cell.

The output of the linear load cell itself is calibrated using a set of precision weights; the force produced by these weights on the load cell is derived from Newton's second law of motion, $F = Mg$, with $g = 9.8m/s^2$. The voltage output of the load cell is post-processed to match the corresponding unit of Newtons by applying a simple linear transformation of the form $y = qx + s$, where q equals the voltage gain and s equals the voltage offset.

3. A SIMPLIFIED PHYSICAL MODEL FOR HAIR RIBBON DEFLECTION

In this section we present a simplified physical model of a flexible thread or hair as appearing in a violin bow, and then we extend it to the case of multiple hairs and generalize it to describe the complete hair ribbon. We use such physical model in order to approximate, given solely information extracted from 6DOF sensors, the force exerted on the string regardless of the displacement or tilting of the bow. An important simplification was to assume the bow stick as rigid.

3.1 The thread

The simplest approximation of the bow hair-ribbon is a single elastic thread stretched between two points A and B (see Figure 3). At its rest position the thread has a length of l, which coincides with the distance between the points A and B. When a force is applied on a point C, the thread stretches and is elongated until an internal equilibrium of the system is reached.

In its rest position, we consider such thread as the limit of an array of masses connected by springs, presenting a mass-to-mass distance approaching zero. We parameterize the thread by a function $u : [0, 1] \rightarrow \mathbb{R}^2$, and express the potential energy of the thread as

$$\frac{1}{2}\frac{T}{l}\int_0^1 u'(t)^2 dt, \qquad (1)$$

where T is the tension of the thread. If u is the parametriza-

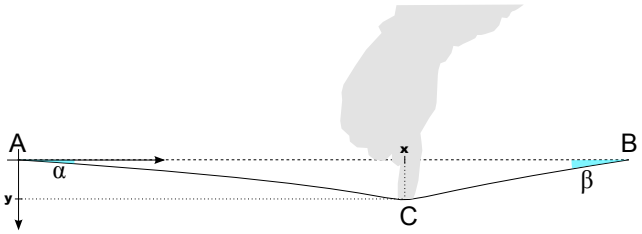

Figure 3: A single elastic thread fixed at two extremes A and B is stretched by applying a force in a point C.

tion of the thread of Figure 3 with $u(0) = A$, $u(c) = C$, and $u(1) = B$ where $c \in]0, 1[$, the potential energy is given by

$$\frac{1}{2}\frac{T}{l}\left(\frac{x^2+y^2}{c} + \frac{(1-x)^2+y^2}{1-c}\right). \tag{2}$$

The internal equilibrium, i.e. the minimum potential energy, is reached for $c = c_{\text{eq}}$, where

$$c_{\text{eq}} = \frac{x^2+y^2}{x^2+y^2+\sqrt{((l-x)^2+y^2)\,(x^2+y^2)}}. \tag{3}$$

In this equilibrium state, the point C is subject to two forces $\overrightarrow{f_1}$ and $\overrightarrow{f_2}$ in the direction CA and CB respectively. Their magnitude is the following:

$$\|\overrightarrow{f_1}\| = T\,(l_1 - c_{\text{eq}} l) \tag{4}$$

$$\|\overrightarrow{f_2}\| = T\,(l_2 - (1 - c_{\text{eq}})\,l) \tag{5}$$

Let's denote l_1 and l_2 the length of the AC and CB parts respectively, α and β the angles CAB and ABC respectively, and $\Delta l = l_1 + l_2 - l$ the total en-lengthening of the thread. The total force that the thread exerts on C is $\overrightarrow{F} = \overrightarrow{f_1} + \overrightarrow{f_2}$. If we set a coordinate system at the center of the thread as shown in Figure 4, the point C will be described by its coordinates (x, y). Now, writing $\overrightarrow{F} = (F_{\text{horz}}, F_{\text{vert}})$ where F_{horz} is the horizontal component of $\overrightarrow{F}$ and F_{vert} the vertical component, the vertical component of the force can be considered as the force applied to the string, and written (observing that $\sin(\alpha) = \frac{y}{l_1}$ and $\sin(\beta) = \frac{y}{l_2}$) as

$$F_{\text{vert}}(x, y) = \|\overrightarrow{f_1}\|\frac{y}{l_1} + \|\overrightarrow{f_2}\|\frac{y}{l_2}. \tag{6}$$

3.2 The Hair Ribbon

A more precise approximation of the hair ribbon is to consider it as a a strip of parallel threads, assuming that the force exerted by the ribbon is the sum of the contributions of each thread. Considering an homogeneous distribution of threads determined by a constant ρ and if we define w to be the width of the strip, we can define the force applied to the string as

$$\text{Force} = \rho \int_0^w f(z)dz, \tag{7}$$

where $f(z)$ is the force density of the thread situated at position z on the strip.

Let $m := y(0)$ and $M := y(w)$ be respectively the measured left-hand side and right-hand side *bow-string distance* (see Section 2.1). We then have

$$y = m + \frac{(M-m)}{w}z. \tag{8}$$

Figure 5 schematically depicts the possible relative positions (displacements) that we considered for the hair ribbon

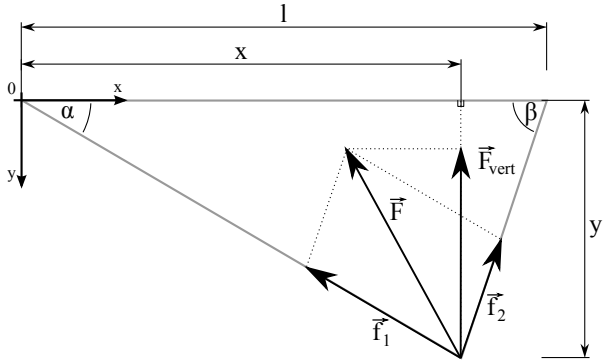

Figure 4: Schematics of the single thread as in Figure 3. The chosen coordinate system is shown in the upper left corner. Note that the y-axis increases towards the bottom. The reaction forces of the threads are drawn. The angles α and β have been exaggerated in the picture so that also the length y and all the force components could be clearly visible.

(transversal view) as relative to the string. The displacement of the string with respect to the bow is determined by the linear relation 8. Only the threads where y is positive are contributing to the force (as they are in contact with the string). This happens[2] when $z > -\frac{wm}{M-m} =: \psi$. Having the diagram of Figure 4 as a reference, we considered the variable x as constant with respect to z while, depending on the changes of y, we reduce the problem to three main cases, defined as

Case I : The y are negative (the ribbon is not touching) with respect to all $z \in [0, w]$, having

$$f(z) = 0\ \forall z; \tag{9}$$

Case II : y is positive for $0 < z < \psi < w$ reaches 0 for $z = \psi$ and is negative for $z > \psi$, with

$$f(z) = \begin{cases} 0 & \text{for } z \in [0, \psi] \\ F(x, y(z)) & \text{for } z \in (\psi, w] \end{cases}; \tag{10}$$

Case III : y is positive for all $z \in [0, w]$, so

$$f(z) = F(x, y(z)). \tag{11}$$

Case I is of little significance, since the force is zero. In the other two cases, applying equation (8) in the equations (10) and (11), we may completely rewrite equation (7) using the definition of f and Δl canceling thus all the indirect dependencies to the variable y. Applying then the substitution $z = \frac{w}{M-m}(y - m)$ to the integral we can write the results in term of the function

$$\tilde{F}(z) := \frac{1}{T}\int_0^z F_{\text{vert}}(x, y)dy, \tag{12}$$

where we divide by T so that $\tilde{F}$ do not depend on the tension. We will handle this parameter in the further formulas.

For the fundamental theorem of calculus plus taking into account the term $\frac{w}{M-m}$ of the substitution, we conclude, for the three considered cases, as

Case I : The y are negative (the ribbon is not touching) with respect to all $z \in [0, w]$, thus

$$\text{Force} = 0;$$

[2]Considering, for the moment, the case where $M > m$ without any loss of generality.

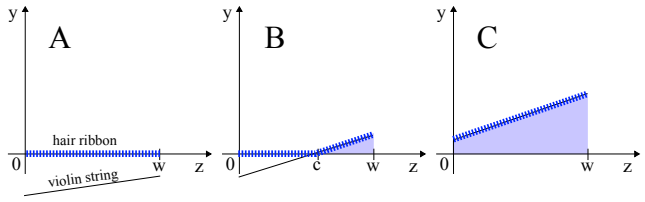

Figure 5: I. Non touching ribbon. II. Partially touching. III. Fully touching.

Case II : y is positive for $0 < z < \psi < w$ reaches 0 for $z = \psi$ and is negative for $z > \psi$, having

$$\text{Force} = T\rho w \frac{\tilde{F}(\max(M,m)) - \tilde{F}(0)}{|M-m|}; \qquad (13)$$

Case III : y is positive for all $z \in [0, w]$, so

$$\text{Force} = T\rho w \frac{\tilde{F}(M) - \tilde{F}(m)}{M-m}. \qquad (14)$$

Finally, we observe that:

1. The final force **only** depends on the variables x, M and m plus the constants T, ρ and w.

2. The cases I, II and III can be identified only looking at M and m. Case I holds when both are negative, case II when they differ in sign and case III when both are positive.

3. Considering $M > m$ did not cause a loss of generality. Indeed, for $M < m$, due to a symmetry of the problem, we could just switch M with m but this, thanks to the way equation (13) has been expressed, does not change the result. Finally we can interpret the case $M = m$ as a limit case of equation (14) when $(M - m) \to 0$. The results of the limit is, in fact, $\text{Force} = \rho w F_{\text{vert}}(x, M)$ corresponding to an equal contribution of all the threads to the final force.

4. OPTIMIZATION PROCEDURE

The described model is parametrized by a single scalar value given by the product $T\rho w$. Changing this parameter will affect the whole prediction, scaling it by a factor. Thus, our initial idea was to infer this factor from an experiment; however, there are additional conditions in the real case which are not addressed by the physical model. First, the motion tracking sensor placed on the bow stick might rotate by a small angle θ after the calibration has been performed, causing a rotation of all the data. Secondly, due to the movement of the sensor, it might be necessary to adjust the offsets of the bow displacement adding a constant a, and the offset of the vertical distance with a constant b. Finally, in order to address the problem of the bending of the stick, another constant r is added defining a transformation which will compensate, the effect of the stick bending by dividing the pseudoforce by a value depending on the bow displacement. The final transformation is given by the following formula:

$$\begin{cases} x' = & a + x \\ M' = & Map_{(x,b,\theta,r)}(M) \\ m' = & Map_{(x,b,\theta,r)}(m) \end{cases}, \qquad (15)$$

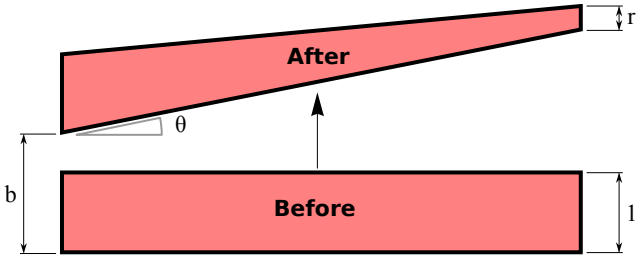

Figure 6: The function Map applied to a rectangle. For this example exaggerated parameters used are $r = 0.5$, $b = 1.5$, $\theta = 0.1$rad.

where

$$\text{Map}_{(x,b,\theta,r)}(y) := (b + y\left(\frac{1+r}{2} + \frac{(-1+r)\left(-\frac{l}{2}+x\right)}{l}\right)\text{Cos}[\theta] + x\text{Sin}[\theta]) \qquad (16)$$

In Figure 6 it is illustrated how the defined transformation alters a rectangle with some fixed inflated parameters.

4.1 Description

Suppose we have a training set $\{(x_i, M_i, m_i)\}_{i=1,\dots,n}$ where x_i is the bow displacement, M_i is the pseudo-force of left side and m_i is the pseudo-force of right side at time i. Given the parameters T, θ, a, b and r we consider the prediction

$$\text{Force}_i(T,\theta,a,b,r) = \text{Force}(x_i + a, \text{Map}_{(x_i,b,\theta,r)}(M_i), \text{Map}_{(x_i,b,\theta,r)}(m_i)). \qquad (17)$$

We want to find the better values for the parameters in order to minimize the absolute error:

$$J(T,\theta,a,b,r) = \frac{1}{2}\sum_{i=1}^{n} (\text{Force}_i(T,\theta,a,b,r) - \text{nidaq}_i)^2. \qquad (18)$$

We thus aim at finding:

$$(T^*,\theta^*,a^*,b^*,r^*) = \underset{(T,\theta,a,b,r)}{\arg\min}\ J(T,\theta,a,b,r) \qquad (19)$$

We use the Nelder-Mead simplex method [6] in order to find a local minimum, starting from the identity transformation parameters: $T = r = 1$, $\theta = a = b = 0$. In order to reduce the computation time, we down-sampled the signal to 8 samples a second. Before the optimization of the parameters we also filtered the dataset, to remove noisy data. We removed the samples where the measurement of the Force cell was less than 0.2. In fact the sensitivity of the sensor for small forces is reduced and noisy.

4.2 Results

Using the acquired gesture parameters along with the Force cell data, we recorded three evaluation datasets. In the *dataset 1*, an almost constant force was applied with different bow transversal positions and different tilts. In the *dataset 2*, the pseudo-force was changing constantly from positive to negative while changing tilt and bow transversal position in order to simulate the way violin is normally played. In the *dataset 3*, bow transversal positions was kept fixed while the force and the tilt where changing. This was done for many different bow transversal positions. Each recording was around one minutes long. We created an *Joint Dataset*, with the samples of the three recordings and

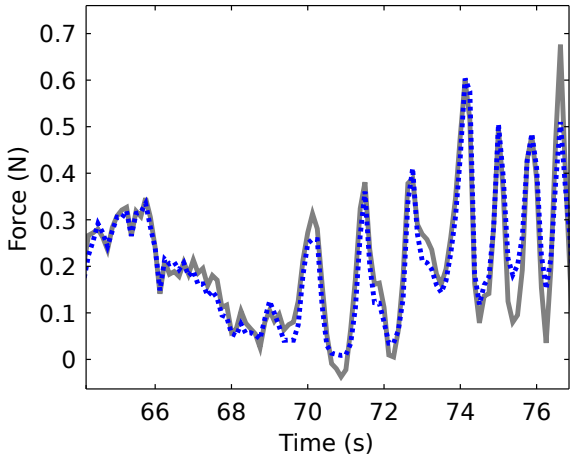

Figure 7: An excerpt of the recorded force signal *(continuous gray line)* along with its prediction *(blue dashed line)* after the optimization has been performed.

we performed a 10-fold cross validation, with a performance going to 13.75 relative error.

Finally, in order to investigate on the best calibration procedure, we also compared the three different datasets. The table 1 shows the results of each possible combination of training-set with test-set. Is clearly shows that even though the second dataset performs best to predict the rest (with 97.4 mean correlation) the other two datasets give comparable results. So even though trying to replicate the variability of parameters of a real performance in the calibration lead to slightly better results, even a short calibration of one minute, with static bow displacement positions results to be good for a general purpose force estimation.

5. CONCLUSION

We presented a physical model of the violin bow assuming a rigid bow stick. We estimated the force of the bow on the string for each configuration of the hairs considering the bow transversal position and the bow-string-distance at the left and right sides of the hair ribbon. We sampled some datasets from with the Polhemus equipment encountering systematic parallax-like errors in the data caused by human error in the calibration procedure or by the sensors. We defined a transformation to correct those effect dependent on 4 parameters. We thus used the training datasets to fit the transformation parameters plus the the tension T of the hairs.

The bow model gives an estimation of the bowing force in Newtons with a very high correlation coefficient for the half of the bow near to the frog. Additionally, by comparing different datasets corresponding to different types of bowing, we are able to identify the type of data that is sufficient for obtaining a good prediction. This way we found out a procedure to calibrate the model in a few seconds.

The main application of this bow physical model is to complement a sensing system for the acquisition of bowing gestures by providing accurate measurements of the force that the bow is exerting on the string while allowing for less intrusive capturing devices. Additionally, the model can be used to build or improve data acquisition for sound controlling interfaces.

Table 1: Relative error and Correlation of the prediction with the true force for each training set and test set coupling.

		Test Set							
		Dataset 1		Dataset 2		Dataset 3		Joint	
Training Set	Dataset 1	corr	rel	corr	rel	corr	rel	corr	rel
		89.21	16.75	96.18	23.68	98.84	14.67	97.29	17.03
	Dataset 2	corr	rel	corr	rel	corr	rel	corr	rel
		95.03	13.78	97.76	16.75	98.37	20.13	97.4	16.88
	Dataset 3	corr	rel	corr	rel	corr	rel	corr	rel
		84.95	23.61	95.87	22.64	98.88	12.18	96.13	19.82
	Joint	corr	rel	corr	rel	corr	rel	corr	rel
		94.1	13.04	97.3	19.73	98.94	12.19	98.12	13.75

6. FUTURE WORK

A clear potential improvement that will be carried out in the future is the estimation of the stick bending effect. By looking at histograms of bow displacement in real playing, we observed that musicians use the lower part of the bow (closer to the frog) significantly more often, which reduces the stick bending effect. When evaluating our model for extreme cases in which the majority of the frames were recorded when the performer was playing near the tip, the performance gets significantly reduced. This could be explained by the fact that in our model we did not address explicitly the effect of the stick bending. The effect is, actually, too big there to be corrected from the mapping in that region of the bow. A further step will be to include the deflection of the string in the model. Such a study should lead to a complete force estimation system for all the parts of the bow while providing a completed physical model of the bow. Such a model will, of course, improve obtained results. However, because of the non-linearity of the model, the precision of the prediction varies according to the bow displacement. This has to be considered an intrinsic limitation of any deflection model of the bow and, as suggested by a reviewer, a thorough study on the propagation of noise in the formulas should be carried out in the future.

Regarding the parallax error arising from the Polhemus equipment, it would be interesting to reproduce the experiment with other type of measurement such as IR camera-based MOCAP (Qualysis) for a comparison of the prediction error.

7. ACKNOWLEDGEMENTS

This work was supported by the EU FP7 FET SIEMPRE Project.

8. REFERENCES

[1] A. Askenfelt. Measurement of bow motion and bow force in violin playing. *The Journal of the Acoustical Society of America*, 80(4):1007–1015, October 1986.

[2] L. Cremer. *Physics of the Violin*. The MIT Press, Cambridge, Massachusetts, USA, November 1984.

[3] M. Demoucron, A. Askenfelt, and R. Causse. Measuring bow force in bowed string performance: Theory and implementation of a bow force sensor. *Acta Acustica united with Acustica*, 95(4):718–732, 2009.

[4] M. Demoucron and R. Caussé. Sound synthesis of bowed string instruments using a gesture based control of a physical model. In *Proceedings of the 2007 International Symposium on Musical Acoustics*, Barcelona, 2007.

[5] E. Guaus, J. Bonada, E. Maestre, A. Perez, and

M. Blaauw. Calibration method to measure accurate bow force for real violin performances. In G. Scavone, editor, *International Computer Music Conference*, pages 251–254, Montreal, Canada, 16/08/2009 2009. The International Computer Music Assiciation, The International Computer Music Assiciation.

[6] J. Lagarias, J. Reeds, M. Wright, and P. Wright. Convergence properties of the Nelder-Mead simplex method in low dimensions. *SIAM Journal on Optimization*, 9(1):112–147, 1999.

[7] E. Maestre, J. Bonada, M. Blaauw, A. Perez, and E. Guaus. Acquisition of violin instrumental gestures using a commercial emf device. In *International Computer Music Conference*, Copenhagen, Denmark, 27/08/2007 2007.

[8] J. A. Paradiso and N. A. Gershenfeld. Musical applications of electric field sensing. *Computer Music Journal*, 21(2):69–89, 1997.

[9] N. Rasamimanana. Gesture analysis of bow strokes using an augmented violin. Master's thesis, IRCAM, Paris, Fance, 2003.

[10] E. Schoonderwaldt. *Mechanics and acoustics of violin bowing*. PhD thesis, Stockholm Royal Institute of Technology, Stockholm, Sweden, 2009.

[11] E. Schoonderwaldt and M. Demoucron. Extraction of bowing parameters from violin performance combining motion capture and sensors. *The Journal of the Acoustical Society of America*, 126(5):2695–2708, 2009.

[12] D. S. Young. Wireless sensor system for meassurement of violin bowing parameters. In *Proceedings of the Stockholm Music Acoustics Conference*, Stockholm, Sweden, 2003.